AIP | Applied Physics Letters

Laser-excited optical emission response of CdTe quantum dot/polymer nanocomposite under shock compression

Pan Xiao, Zhitao Kang, Alexandr A. Bansihev, Jennifer Breidenich, David A. Scripka, James M. Christensen, Christopher J. Summers, Dana D. Dlott, Naresh N. Thadhani, and Min Zhou

Citation: Applied Physics Letters **108**, 011908 (2016); doi: 10.1063/1.4939701
View online: http://dx.doi.org/10.1063/1.4939701
View Table of Contents: http://scitation.aip.org/content/aip/journal/apl/108/1?ver=pdfcov
Published by the AIP Publishing

Laser-excited optical emission response of CdTe quantum dot/polymer nanocomposite under shock compression

Pan Xiao,[1,2] Zhitao Kang,[3] Alexandr A. Bansihev,[4] Jennifer Breidenich,[5] David A. Scripka,[5] James M. Christensen,[4] Christopher J. Summers,[3] Dana D. Dlott,[4] Naresh N. Thadhani,[5] and Min Zhou[2,5,a)]

[1]*LNM, Institute of Mechanics, Chinese Academy of Sciences, Beijing 100190, China*
[2]*George W. Woodruff School of Mechanical Engineering, Georgia Institute of Technology, Atlanta, Georgia 30332-0405, USA*
[3]*Phosphor Technology Center of Excellence, Georgia Tech Research Institute, Georgia Institute of Technology, Atlanta, Georgia 30332-0826, USA*
[4]*School of Chemical Sciences and Frederick Seitz Materials Research Laboratory, University of Illinois at Urbana-Champaign, Urbana, Illinois 61801, USA*
[5]*School of Materials Science and Engineering, Georgia Institute of Technology, Atlanta, Georgia 30332-0245, USA*

(Received 29 October 2015; accepted 28 December 2015; published online 8 January 2016)

Laser-driven shock compression experiments and corresponding finite element method simulations are carried out to investigate the blueshift in the optical emission spectra under continuous laser excitation of a dilute composite consisting of 0.15% CdTe quantum dots by weight embedded in polyvinyl alcohol polymer. This material is a potential candidate for use as internal stress sensors. The analyses focus on the time histories of the wavelength blue-shift for shock loading with pressures up to 7.3 GPa. The combined measurements and calculations allow a relation between the wavelength blueshift and pressure for the loading conditions to be extracted. It is found that the blueshift first increases with pressure to a maximum and subsequently decreases with pressure. This trend is different from the monotonic increase of blueshift with pressure observed under conditions of quasistatic hydrostatic compression. Additionally, the blueshift in the shock experiments is much smaller than that in hydrostatic experiments at the same pressure levels. The differences in responses are attributed to the different stress states achieved in the shock and hydrostatic experiments and the time dependence of the mechanical response of the polymer in the composite. The findings offer a potential guide for the design and development of materials for internal stress sensors for shock conditions. © *2016 AIP Publishing LLC*. [http://dx.doi.org/10.1063/1.4939701]

The shock compression of highly heterogeneous materials such as particulate media results in dynamic response that is dominated by meso-scale processes whose conditions, especially states in the interior of the materials, are difficult to measure directly. There is a great need for stress sensing materials (SSM) that can provide time-resolved quantification of conditions inside the materials with no or as little intrusion as possible. Particle-level sensing in shock experiments requires the SSM to be small in size and possesses stress-dependent physical properties (e.g., optical properties) whose signal(s) can be captured and recorded as quickly as possible to achieve high temporal resolutions.[1–3] Traditional SSMs, such as strain gauges and piezoresistive/piezoelectric materials, can provide time resolutions down to the nanosecond scale but have spatial resolutions spanning an area of the sensor element of several millimeters. Hence, they are excellent for obtaining continuum-scale measurements representing the average response of a sample volume. Quantum dots (QDs), with diameters ranging from several to a hundred nanometers, exhibit unique optical properties due to the quantum confinement effect.[4] Their optical properties are reported to be pressure-dependent.[5,6] Therefore, QDs can potentially be used for time-resolved stress sensing in the study of meso-scale particle-level responses in shock experiments. Although photoluminescence (PL) of QDs under hydrostatic compression has been widely studied,[7–9] less is known about their response under shock compression. In the present work, the optical response of nanocomposite films consisting of CdTe QDs and polymer polyvinyl alcohol (PVA) under laser-driven shock compression was investigated to seek the possibility of utilizing CdTe QDs as SSMs in shock experiments.

The QD/PVA composite was prepared with the method reported by Kang *et al.*[10,11] The particular PVA used is Airvol 523. Under ambient conditions, the PL emission of the QDs shows a peak wavelength around 586 nm (Fig. 1(c) for $t = 0$), indicating the size of the QDs to be ~3 nm. The concentration of the QDs in the PVA is about 0.15 wt. %. The sample shown in Fig. 1(a) is made by drop-coating a ~30 μm thick QD/PVA composite film onto a glass substrate of $25.4 \times 25.4 \times 0.5$ mm in dimensions. Shock compression experiments on the QD/PVA samples are performed with the laser-driven shock system developed by the Dlott group.[12,13] The same experimental set-up reported in Ref. 14 is used, but the material arrangement of the samples is different. As depicted in Fig. 1(b), an aluminum (Al) flyer plate is launched off of a 50 μm thick glass-Al foil with a spatially homogenized laser pulse.[15] The diameter of the launch laser pulse is about 700 μm, while the diameter of the central flat

a)Author to whom correspondence should be addressed. Electronic mail: min.zhou@gatech.edu. Tel.: 404-894-3294. Fax: 404-894-0186.

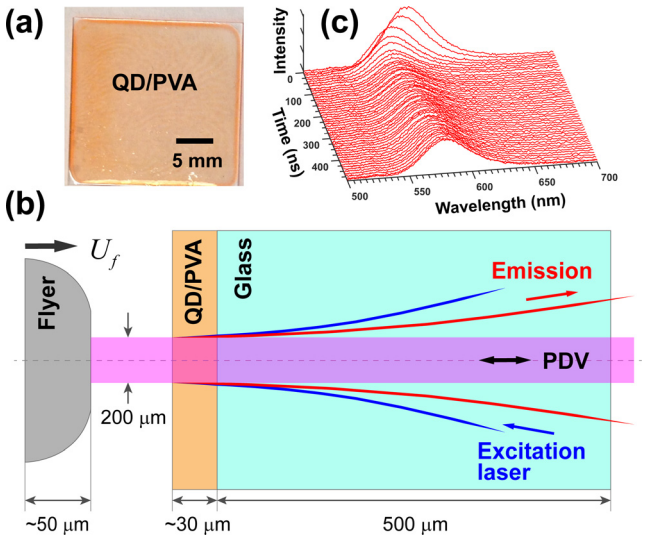

FIG. 1. (a) A CdTe QD/PVA sample used in experiment; (b) schematic illustration of the target, QD/PVA film, glass substrate, and probe beams; and (c) a typical time stream emission spectra from the QD/PVA composite under shock compression.

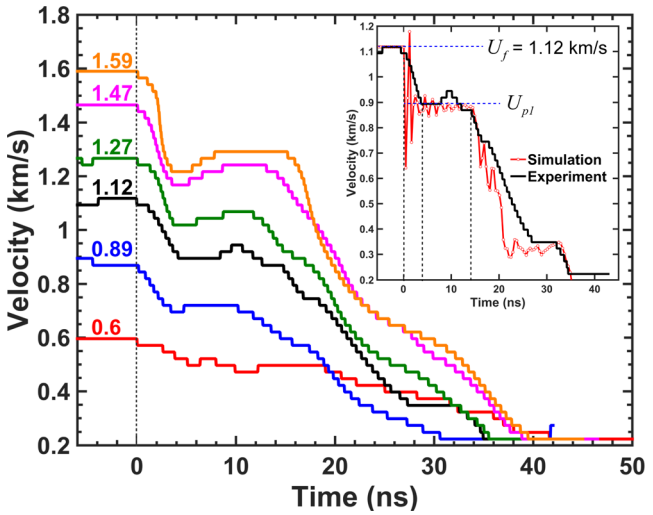

FIG. 2. Velocity histories obtained from the PDV at different initial flyer velocities (U_f). *Inset*: measured and calculated velocity histories for $U_f = 1.12$ km/s.

region is about 500 μm, of which only the 200 μm central region is probed.[15] The flyer plate velocity is controlled by the energy of the launch laser pulse and measured using photonic Doppler velocimetry (PDV). Emission of the QDs is induced by ~250 ns pulses with a wave length of 527 nm from a Q-switched Nd:YLF excitation laser.[14] The emission spectra are detected at 0.5 ns time intervals using a streak camera.[12,14] A typical time stream of emission spectra is shown in Fig. 1(c). The sheet is used to generate flyers and the sample target includes large, uniform surfaces. After a flyer is punched out from the sheet by the laser beam for one shot, the sheet and the target are translated to a new, fresh region for the next shot for which a new flyer is generated and launched at new initial velocities (U_f) onto the target.

In conjunction with the experiments, the shock compression of the CdTe QD/PVA film is also analyzed using finite element method (FEM) simulations in order to quantify the distribution and evolution of the internal pressure in the samples. The dimensions in the simulation model are similar to those in the experiments. The equation-of-state (EOS) with parameters from Ref. 16 is used to describe the volumetric response of the Al flyer and the QD/PVA composite film. The Johnson-Cook model with parameters from Ref. 17 is used to describe the viscoplastic behavior of the flyer plate. The elasticity model with parameters from Ref. 18 is used to model the glass substrate. The QD/PVA film adhered on the glass substrate is impacted by the flyer with velocity U_f which is determined from the PDV measurement. We focus on pressure distribution in the central region of the QD/PVA film with a diameter of 200 μm which corresponds to the laser illuminated region in the experiments. The FEM simulations are carried out using the commercial package Abaqus.

Fig. 2 shows the velocity histories of the flyer plates as measured by the PDV in the experiments with different launch laser energies. The initial flyer velocities after launching range from 0.60 to 1.59 km/s. After contact between the flyer and the PVA film at $t = 0$ ns, the PDV monitors the velocity U_p of the flyer/PVA interface. All the velocity profiles in Fig. 2 show similar variation trends. Take $U_f = 1.12$ km/s for example, (inset in Fig. 2), the velocity drops precipitously from $U_f = 1.12$ km/s to $U_{p1} = 0.89$ km/s within a time period of $\tau_{drop} = 4$ ns. The velocity U_{p1} is maintained for a duration of about 11 ns (denoted as τ_{p1}) before the deceleration stage starts. The existence of τ_{drop} is due to the tilt between and roughness of the impact surfaces. Data suggest the effects take place over approximately 4 μm. It can be seen that as U_f increases from 0.60 to 1.59 km/s, U_{p1} increases from 0.49 to 1.29 km/s (as listed in Table I).

The velocity profile from a simulation with $U_f = 1.12$ km/s is also plotted in the inset of Fig. 2 and shows agreement with the PDV data. The sharper decrease after the contact in the simulation is due to the fact that the contacting surfaces of the flyer and the QD/PVA film are assumed to be ideally smooth and parallel. In the simulations, the velocity stays at U_{p1} for a duration of approximately 15 ns, while the deceleration stage starts essentially at the same time as in the experiments. To illustrate how the shockwaves propagate in the flyer and target, a time-position diagram extracted from the simulations is shown in Fig. 3. Several key time scales are worth noting. $\tau_{s1-PVA} = 9.1$ ns is the time for the initial shockwave to propagate from the flyer/PVA interface to the PVA/glass interface. $\tau_{r1-PVA} = 5.8$ ns is the time for the reflected shockwave from the PVA/glass interface to propagate back to the flyer/PVA interface. Reflecting these times, U_{p1} lasts for approximately 15 ns ($\tau_{s1-PVA} + \tau_{r1-PVA}$) before the first reflected wave in the PVA reaches the flyer/PVA interface. The round trip time in the flyer is about 20 ns

TABLE I. Particle velocity (U_{p1}), arrival time at PVA/glass interface (τ_{s1-PVA}) for initial shock wave, and pressure estimated from the Rankine-Hugoniot relation (P_s) at different initial flyer velocities (U_f).

U_f (km/s)	0.60	0.89	1.12	1.27	1.47	1.59
U_{p1} (km/s)	0.49	0.72	0.89	1.07	1.24	1.29
τ_{s1-PVA} (ns)	10.8	9.8	9.1	8.5	7.9	7.8
P_s (GPa)	2.0	3.3	4.3	5.6	6.9	7.3

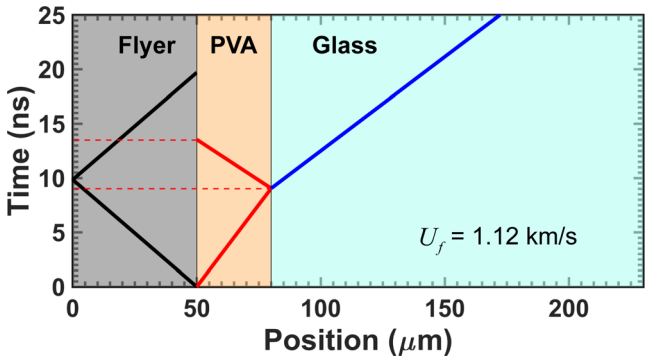

FIG. 3. Time–position diagram for one-dimensional propagation of shock and reflection waves in different materials.

which is longer than that in the film. It takes about 86.2 ns for the shockwave to propagate from the PVA/glass interface to the bottom of the glass substrate. Finally, the time it takes for release waves to propagate from the side corner of the flyer to the center of the PVA/glass interface is approximately 10 ns, but this is not the time for the release wave to reach the excited region which happens later. A comparison of all the time scales shows that the laser illuminated region of the PVA film is under a relative homogenous state of stress at $t = \tau_{s1-PVA}$ when the other reflected waves have not yet reached the region. The time τ_{s1-PVA} for experiments at other U_f values are listed in Table I.

The time stream of emission spectra for $U_f = 0.6$ and 1.12 km/s is shown in Figs. 4(a) and 4(b), respectively. It can be seen that the emission intensity peak shifts from the initial wavelength of 586 nm towards the shorter wavelength region (blueshifting) after the onset of loading. CdTe is a direct band gap semiconductor with strong quantum confinement effect in nanometer size samples. As the QDs are compressed, the interatomic spacings and the size of the QDs in the direction of loading decrease, leading to increases in band gap energy and the blueshift of wavelength.[7,9] Therefore, the blueshift can be used as an indicator and measure for the internal stress during shock loading. The emission spectra at different values of U_f are processed using the method proposed by Brown *et al.*,[12] to extract the average wavelength histories ($\lambda(t)$). The blueshift histories are calculated as $\Delta\lambda(t) = \lambda(0) - \lambda(t)$ and plotted in Fig. 4(d). Variations in the blueshift histories are rather complicated. Specifically, for $U_f = 0.60$ km/s, the blueshift increases to a maximum ($\Delta\lambda_{max}$) of 8.9 nm at around 50 ns and then decreases gradually. The blueshift history for $U_f = 0.89$ km/s shows a similar trend, with a larger $\Delta\lambda_{max}$ of 14.5 nm. However, as U_f increases to 1.12 km/s, the blueshift first increases to $\Delta\lambda_{max} = 15.2$ nm at about 30 ns and then decreases to 13.5 nm at about 48 ns; after that it increases again to a second maximum value ($\Delta\lambda'_{max}$) of 18.5 nm at around 64 ns. As U_f further increases to 1.59 km/s, blueshift histories show a variation trend similar to that for $U_f = 1.12$ km/s, but both $\Delta\lambda_{max}$ and $\Delta\lambda'_{max}$ decrease with U_f. Apparently, $U_f = 1.12$ km/s is a critical velocity, below and above which the blueshift variation trend is different. Similar trends are observed with other samples of the same QDs/PVA composition.

To understand the shock-induced blueshift response, the pressure distribution and evolution in the excited QD/PVA region from a simulation with $U_f = 1.12$ km/s is shown in Fig. 5(a). At the early stage for each shot, the shockwave with constant pressure P_s moves at shock velocity U_s in the QD/PVA film, taking about τ_{s1-PVA} to traverse the film. The shock pressure and velocity in the film can be estimated from the famous Rankine-Hugoniot relation[12,16]

$$\begin{aligned} U_s &= a + bU_p \\ P_s - P_0 &= \rho_0 U_s U_p, \end{aligned} \tag{1}$$

where U_p is the particle velocity which is measured with PDV in the experiment; ρ_0 is the density of the film material; and $a = 2.46$ km/s and $b = 1.565$ are constants obtained from the experiments.[16] The shock pressure (P_s) values calculated

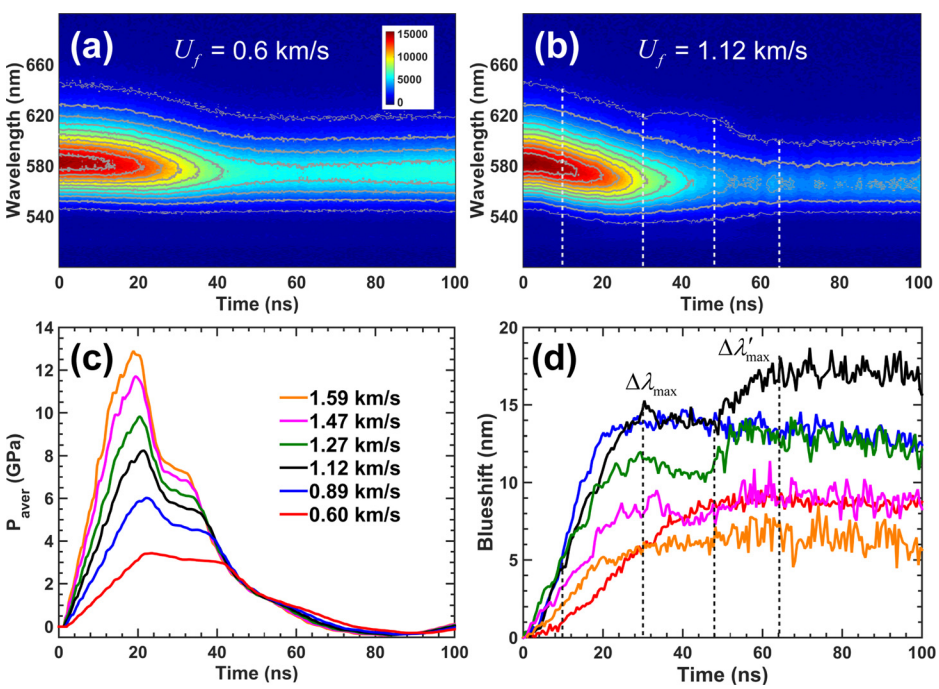

FIG. 4. Emission spectra for (a) $U_f = 0.6$ km/s and (b) $U_f = 1.12$ km/s, the contour colors indicate emission intensity; (c) average pressure obtained from simulations; and (d) blueshift histories at different U_f from shock experiments.

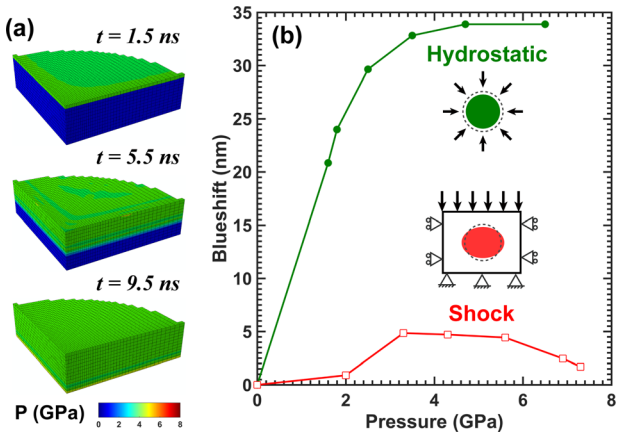

FIG. 5. (a) Calculated pressure distributions in the excited region of a QD/PVA composite sample for $U_f = 1.12$ km/s; (b) pressure-dependent blueshifts of QD/PVA composite obtained from quasistatic hydrostatic and shock compression experiments. *Inset*: different strain states of the QDs under hydrostatic and shock (overall composite uniaxial strain) compression.

from Eq. (1) are listed in Table I. Alternatively, P_s and U_s are also obtained from FEM simulations and found to be very close to that calculated from Eq. (1). At $t = \tau_{s1-PVA}$ when the excited region is in uniform pressure states, the blueshift $\Delta\bar{\lambda}(t)$ obtained from the shock experiments corresponds to the average blueshift of all the QDs at pressure P_s. Therefore, the relation between blueshift $(\Delta\bar{\lambda}(t))$ and shock pressure (P_s) can be obtained based on the experiment and simulation results at $t = \tau_{s1-PVA}$, which is plotted in Fig. 5(b). The average pressure histories in the excited region under shock loading at different values of U_f are plotted in Fig. 4(c). During loading, the average pressure values increase to a maximum $(\bar{P}_{\max})$ at times between 20 and 25 ns. It can be seen from Fig. 4(c) that $\bar{P}_{\max}$ increases monotonically with U_f. After $\bar{P}_{\max}$, the calculated average pressure decreases to 0 GPa within 100 ns.

For comparison, the emission spectra of the QD/PVA composite are also examined under quasistatic compression in a diamond anvil cell. The measured pressure-blueshift relation is also shown in Fig. 5(b). The blueshift from the hydrostatic experiment increases monotonically to 35 nm as the pressure increases to 6.5 GPa. After that the PL fluorescence disappears, indicating a possible phase transformation of the CdTe QDs from zinc-blende to rock-salt structure.[9] It can be seen in Fig. 5(b) that the blueshift-pressure relation for shock compression is quite different from that for hydrostatic compression under quasistatic rate. The following salient points highlight the differences: (1) unlike the monotonic increase under hydrostatic compression, the blueshift under shock compression first increases to a maximum of 5.2 nm at 4.3 GPa and subsequently decreases to 1.6 nm at 7.3 GPa; (2) the maximum blueshift (about 18 nm) obtained for shock compression is smaller than the maximum blueshift (35 nm) observed for hydrostatic compression; (3) no obvious evidence of phase transformation is observed at the early stage $(t \le \tau_{s1-PVA})$ of the emission spectra, since fluorescence did not disappear suddenly; and (4) an analysis of the blueshift histories and pressure distribution indicates that the blueshift in shock compression as shown in Fig. 4(d) cannot be explained with a single blueshift-pressure constitutive relation. In other words, a velocity- or rate-dependent blueshift-pressure relation should be employed to predict the blueshift response of the QD/PVA composite under shock compression at different values of U_f.

The differences between the pressure-dependent blueshifts from the hydrostatic compression under quasistatic conditions and shock compression can be attributed to different stress states the QDs experience in the two settings.

First, note that the emission spectrum of QDs is determined by their electronic band structure which is dramatically affected by the levels and triaxiality of the strain/stress states in the QDs.[19–21] Specifically, the blueshift of the QDs changes not only with the sign and level of the stress/strain in each of the three spatial directions but also with the ratios between the stresses/strains in the three directions. As illustrated in Fig. 5(b), hydrostatic compression under quasistatic conditions and shock compression have very different stress/strain ratios in the three spatial directions. The former has equal stresses/strains in all directions (ratios are unity). On the other hand, FEM simulations show that under shock compression conditions of uniaxial strain prevail in the overall QD/PVA composite sample in early stages. For such uniaxial strain conditions, additional unit cell calculations with a QD embedded in a matrix [Fig. 5(b)] reveal that the ratio between a QD's strain in the lateral direction (ε_l) and the strain in the impact direction is $\varepsilon_l/\varepsilon_i \approx -0.24$, with $\varepsilon_l > 0$ (lateral dimensions increasing) and $\varepsilon_i < 0$ (longitudinal dimension decreasing). This ratio is quite different from the ratio of 1 for the hydrostatic case. Empirical tight-binding (ETB) calculations reported in a separate publication of blueshift for the CdTe QDs under the two sets of conditions show very similar trends as what is observed in the experiments and shown in Fig. 5 here.[22] Similar dependence band gap energy on strain state is also observed in experiments and simulations in CdSe QDs.[19]

Second, when the QD/PVA composite is subject to impact loading, an instantaneous elastic compression is followed by a gradual relaxation due to conformational changes that continues to increase the local mass density around the QDs.[23] Based on the energy landscape model,[23] the two-stage deformation of QD/PVA composite under shock compression in the nanosecond regime can produce non-uniform stress environments for the QDs. As a result, the non-hydrostatic stress state and non-uniform stresses contribute to the different trends in blueshift.

Third, the mechanical response of the PVA is rate-dependent due to its unique microstructures.[24] This rate-dependence can also affect the blueshift response of QDs at different U_f as it changes the stress states and the time-histories of stresses in the overall material and the QDs. Fully dynamic full-field analyses accounting for this time-dependence are underway to establish a fundamental relation between the blueshift, strain state of the QDs, and stress state of the matrix for shock conditions.

In summary, the optical emission of CdTe QD/PVA composite under shock compression is investigated using laser-driven shock experiments, quasistatic hydrostatic compression, and FEM simulations. The composite film, consisting of polymer PVA (Airvol 523) and ~3 nm CdTe QDs

with concentration of about 0.15 wt. %, is impacted by laser-launched Al flyers. The flyers shock the film with initial velocity ranging from 0.6 to 1.12 km/s, producing uniform pressures ranging from 2.0 to 7.9 GPa throughout the film at the early stage. Analysis of the emission spectra from the shock experiments reveals that the blueshift first increases to a maximum of approximately 5.2 nm at 4.3 GPa and subsequently decreases with pressure. This behavior is quite different from the blueshift response observed in hydrostatic experiments which shows monotonically increasing blueshift with pressure, up to 35 nm at 6.5 GPa. The mechanisms associated with the differences in the blueshift trends can be attributed to the different stress states, stress non-uniformity and time-dependence of the composite behavior. The results indicate that the blueshift of the CdTe QDs can be used as a means for obtaining measurements of local and select area stress/strain conditions in materials with nanosecond resolutions. However, it is important to recognize the stress/stain state dependent nature of the blueshift of the CdTe QDs and the effect of interactions between the QDs and the matrix material, such that material-specific and loading-rate-specific calibrations need to be carried in advance. To this end, the research reported here represents a first step for the CdTe QD/PVA composite and more research and analysis are needed to quantify and calibrate the response. In a broader sense, the development of other SSMs with simpler responses that are rate-independent may be desirable. For example, the use of matrix materials that are less rate-dependent or time-independent may simplify the calibration needed.

The authors gratefully acknowledge support from the Defense Threat Reduction Agency (DTRA) through Grant No. HDTRA1-12-1-0052 at Georgia Tech and HDTRA1-12-1-0011 at UIUC, the National Basic Research Program of China through Grant No. 2012CB937500, the CAS/SAFEA International Partnership Program for Creative Research Teams, and the National Natural Science Foundation of China through Grant No. 11202212, 11432014. Calculations are carried out on parallel computers at DPRL at Georgia Tech and the ScGrid Supercomputing Center of the Computer Network Information Center of the Chinese Academy of Sciences.

[1]D. C. Swift, J. G. Niemczura, D. L. Paisley, R. P. Johnson, S. N. Luo, and T. E. Tierney IV, Rev. Sci. Instrum. **76**, 093907 (2005).
[2]W. M. Trott, AIP Conf. Proc. **620**, 1347–1350 (2002).
[3]R. J. Trainor, J. W. Shaner, J. M. Auerbach, and N. C. Holmes, Phys. Rev. Lett. **42**, 1154 (1979).
[4]W. C. Chan, Science **281**, 2016 (1998).
[5]M. Narayanan and A. J. Peter, Quantum Matter **1**, 53 (2012).
[6]H. G. Drickamer, C. W. Frank, and C. P. Slichter, Proc. Natl. Acad. Sci. U. S. A. **69**, 933 (1972).
[7]E. Pedrueza, A. Segura, R. Abargues, J. B. Bailach, J. C. Chervin, and J. P. Martínez-Pastor, Nanotechnology **24**, 205701 (2013).
[8]Y. Lin, Proc. SPIE **9373**, 93730L (2015).
[9]F. Wu, J. M. Zaug, C. E. Young, and J. Z. Zhang, J. Nanosci. Nanotechnol. **8**, 6528 (2008).
[10]T. Zhang, X. Sun, and B. Liu, Spectrochim. Acta, Part A **79**, 1566 (2011).
[11]Z. Kang, Y. Zhang, H. Menkara, B. K. Wagner, C. J. Summers, W. Lawrence, and V. Nagarkar, Appl. Phys. Lett. **98**, 181914 (2011).
[12]K. E. Brown, Y. Fu, W. L. Shaw, and D. D. Dlott, J. Appl. Phys. **112**, 103508 (2012).
[13]K. E. Brown, W. L. Shaw, X. Zheng, and D. D. Dlott, Rev. Sci. Instrum. **83**, 103901 (2012).
[14]A. A. Banishev, W. L. Shaw, and D. D. Dlott, Appl. Phys. Lett. **104**, 101914 (2014).
[15]A. D. Curtis, A. A. Banishev, W. L. Shaw, and D. D. Dlott, Rev. Sci. Instrum. **85**, 043908 (2014).
[16]S. Chaurasia, P. Leshma, J. Pasley, S. Tripathi, and M. Kumar, Curr. Sci. **103**, 1447 (2012).
[17]N. K. Sanjeev, V. Malik, and H. S. Hebbar, Int. J. Res. Eng. Technol. **3**, 98 (2014).
[18]W. Hu, Y. Wang, J. Yu, C. F. Yen, and F. Bobaru, Int. J. Impact Eng. **62**, 152 (2013).
[19]C. D. Grant, J. C. Crowhurst, S. Hamel, A. J. Williamson, and N. Zaitseva, Small **4**, 788 (2008).
[20]R. Santoprete, B. Koiller, R. B. Capaz, P. Kratzer, Q. K. K. Liu, and M. Scheffler, Phys. Rev. B **68**, 235311 (2003).
[21]E. Groeneveld, C. Delerue, G. Allan, Y.-M. Niquet, and C. de Mello Donegá, J. Phys. Chem. C **116**, 23160 (2012).
[22]P. Xiao, F. Ke, Y. Bai, and M. Zhou, "Compressive deformation-induced blueshift in emission spectrum of CdTe quantum dot/polymer composite" (unpublished).
[23]H. Kim, S. Hambir, and D. D. Dlott, Phys. Rev. Lett. **83**, 5034 (1999).
[24]L. E. Millon, C. J. Oates, and W. Wan, J. Biomed. Mater. Res., Part B **90**, 922 (2009).